Hydrogeology Journal (2021) 29:1539–1550
https://doi.org/10.1007/s10040-021-02327-x

PAPER

A parsimonious approach for large-scale tracer test interpretation

Vincent Bailly-Comte[1,2] · Séverin Pistre[3]

Received: 13 May 2020 / Accepted: 18 February 2021 / Published online: 1 April 2021

Abstract

Dye tracing is an efficient method for spring watershed delineation, but is also used in surface waters to assess pollution migration over several kilometers. The aim of this study is to develop a simple and parsimonious approach that accounts for a linear relationship between dispersivity and scale that could be used for the simulation of large-scale transport processes in aquifers. The analysis of 583 tracer recoveries is used to validate an inverse relationship between arrival time and peak concentration, which is shown to be a consequence of the linear relationship between dispersivity and scale. These results show that the tracer displacement through a given tracing system can be characterized at a large scale by a constant Peclet number. This interpretation is used to propose a new approach for tracer test design based on the analytical expression of the peak/time factor. It is also used for Peclet number assessment and simulation of the whole tracer residence-time distribution using a new method based on the ratio between the mode of the residence time distribution (h_{mod}) and the corresponding time from injection (t_{mod}), which is called the h_{mod}/t_{mod} method. This methodology is applied to two tracer tests carried out in a karst aquifer over 13 km between the same injection and detection points under distinct hydrological conditions. These results found practical applications in generalizing tracer test results to various flow conditions, or guiding the parameterization of physically-based vulnerability mapping methods.

Keywords Tracer test · Residence time distribution · Scale effect · Karst

Introduction

Quantitative analyses of tracer tests provide direct information on processes that control the migration of contaminants. Such techniques have been widely applied in surface water and groundwater hydrology to describe transport processes and assess the vulnerability of rivers or aquifers to contamination, which is of primary importance when considering the protection and management policies of water resources. In addition, tracer tests can provide information on landslide dynamics (Ronchetti et al. 2020) and, along with environmental tracers, they can be used for the conceptualization of groundwater flow and transport (Lauber and Goldscheider 2014), or to improve the numerical groundwater models (Schilling et al. 2019). Dye tracing is also a very effective technique for delineating catchment areas of springs or wells, but the quantitative results of large-scale tracer tests are often poorly exploited in engineering reports. This method would be particularly useful for the parameterization of physically based vulnerability mapping methods, especially in karstified environments (Dedewanou et al. 2015; Popescu et al. 2019). Tracer hydrology is now an important field of research that has found operational application in various hydrosystems at different scales (Field 2002). This means that numerous data, including accurate tracer breakthrough curves expressed as residence time distribution (RTD), can be found in numerous scientific papers and reports. For instance, Labat and Mangin (2015) show how an inverse Laplace-transform procedure applied to a tracer RTD can be used to distinguish a quick-flow advection-dominated component from a slow-flow advection–dispersion/dominated component in a karstic aquifer.

Since the 1960s, many authors have proposed analytical solutions to simulate tracer breakthrough curves for various initial/boundary conditions, using the conceptual framework of the advection-dispersion equation—ADE, see for example Kreft and Zuber (1978), Sauty (1980) or Chatwin (1971). An initial complication in applying this theory was found when tracer tests were carried out over long distances, leading

✉ Vincent Bailly-Comte
v.bailly-comte@brgm.fr

1 BRGM, Univ Montpellier, Montpellier, France

2 G-eau, UMR 183, INRAE, CIRAD, IRD, AgroParisTech, Supagro, BRGM, Montpellier, France

3 Hydrosciences Laboratory, Montpellier University, CNRS, IRD, Montpellier, France

researchers to develop more complex theories of dispersive transport mechanisms in groundwater (see for instance Berkowitz et al. 2006). However, as pointed out by Cvetkovic (2013), most tracer tests carried out to understand the scale effect use less than a 100-m scale, which raises the question of the applicability of these approaches to large-scale experiments, typically 1–10 km for karst systems. In addition, it has been shown that large-scale tracer transport can be reasonably well described, assuming simple advective and dispersive processes (Birk et al. 2005; Massei et al. 2006; Mull et al. 1988), which remains the most parsimonious approach, but the significance of the fitted parameters becomes questionable.

In this context, this study aims to better understand how the relatively simple ADE framework can be used to simulate transport processes at a large scale. As a consequence, the physical concepts that will be discussed in the following are not new, but the amount of data that is now available allows the proposition of new insights to describe large-scale dispersive processes in surface water and groundwater.

This study will first investigate simple relationships between parameters of tracer RTD assuming a Fickian theory of transport and a linear dispersive scale effect. The aim of this work is not to discuss or better understand the origin of a linear relationship between scale and dispersivity, but to use this information to develop a simple way of numerically simulating large (basin) scale transport.

Following this, the consistency of such relationships will be discussed using a sizeable dataset based on an extensive literature review focusing on tracer tests in various geological media. Finally, a discussion will focus on the Peclet number as an intrinsic dimensionless parameter to describe large-scale dispersive properties of surface waters and karstified/porous/fractured aquifers, with application to two tracer tests performed on the same tracing system but in distinct hydrological conditions.

Scientific background

Advection-dispersion equation (ADE)

The ADE governs the spatial and temporal evolution of a solute concentration within a moving fluid. It is based on the flux mass balance of a conservative tracer within a control volume, which gives for one-dimensional cases (Eq. 1; Bear 1972):

$$D\frac{\partial^2 C(x,t)}{\partial x^2} - V\frac{\partial C(x,t)}{\partial x} = \frac{\partial C(x,t)}{\partial t} \quad (1)$$

where D [L^2 T^{-1}] is the dispersion coefficient, V [L T^{-1}] is the (microscopic) flow velocity, i.e. the Darcy velocity for porous media divided by the kinematic porosity, t is time, x is the Cartesian coordinate in the direction of flow and C [M L^{-3}] is the solute concentration. Neglecting molecular diffusion and assuming the Fickian theory of diffusion and kinematic dispersion (Fisher 1967), D is expressed as the product of the flow velocity V with the longitudinal dispersivity α [L] (Bear 1972). This means that D and α are not a function of x, so that α could be seen as an intrinsic property of the medium. It also assumes that the velocity does not depend on the concentration, and that there is no change in density and viscosity of the fluid (de Marsily 1986). The relative effectiveness of advection to hydrodynamic dispersion and diffusion is given by the macroscopic Peclet (Pe) number. This dimensionless number can be computed at a distance ℓ [L] along the flow path as follows (Eq. 2):

$$\mathrm{Pe} = \frac{\ell \times V}{D} \quad (2)$$

Advection is considered to dominate the solute transport processes when Pe > 6.0 (Fetter 1992), which is exceeded for most tracer experiments in nonporous media, and especially in karst conduits.

Experimental evidence of dispersive scaling properties

Numerous experiments show that the longitudinal dispersivity α increases with the travelled distance ℓ (Gelhar et al. 1992; Lallemand-Barres and Peaudecerf (1978); Neuman 1990; Pickens and Grisak (1981) and others that can be found in Schulze-Makuch 2005). As a result, as highlighted by Maloszewski and Zuber (1990), knowledge of the dependence of dispersivity on distance is likely more important than an accurate estimation of local parameters. These previous works show that the apparent longitudinal dispersivity is a function of the experimental scale ℓ of the hydrosystem, but not a function of the variable x that fluctuates between $x = 0$ and $x = \ell$. There is thus no reason to infer that the longitudinal dispersivity varies with x, although this assumption has been successfully used in works dealing with scale-dependent models (Huang et al. 1996; Pang and Hunt 2001).

Dispersivity as a linear function of the scale

Numerous authors discussed the influence of the spatial distribution of hydraulic conductivity within a statistically homogeneous porous or fractured media on the scaling of dispersive properties (Puyguiraud et al. 2019). It is often argued that a small tracer plume explores less heterogeneity than a larger one, which induces an increase of dispersivity with distance travelled (Fadili et al. 1999). According to Lenormand (1995), spreading caused by spatial variation of the velocity field is the main source of macro-dispersion. This is equivalent to the concept of heterogeneous advection used by Becker and Shapiro (2003) to describe mass spreading related to

separation of advective pathways (Berkowitz et al. 2006). The scaling of dispersive properties has also been interpreted as a consequence of the use of a n-1 dimension analytical solution to a n-dimension problem (Pickens and Grisak 1981)—Morel-Seytoux and Nachabe (1992) demonstrated that for permanent flow conditions with pure advection in 2D that an equivalent one-dimensional (1D) macro-dispersivity transport scheme can be used with a dispersivity that will be a linear function of the scale. This work introduces a proportionality factor between macroscopic dispersivity and scale, which was also used by Pickens and Grisak (1981) for well-to-well tracer tests performed in a sandy stratified aquifer. Neglecting molecular diffusion, this dimensionless ratio is equivalent to the dispersion parameter used by Maloszewski and Zuber (1982), which is also called specific dispersivity by Singh (2006). This dispersion parameter equals the inverse of Pe (Eq. 1), which means that the dispersivity can be expressed as the ratio between the length of the flow path and Pe (Eq. 3):

$$\alpha = \frac{\ell}{\mathrm{Pe}} \tag{3}$$

Analytical relationships between parameters of tracer RTD

Theoretical solutions to the ADE

Some analytical relationships between parameters of tracer RTD have been proposed for decades, and particularly between parameters that are useful for assessments of vulnerability to contamination—the mean residence time, the modal time and the peak concentration (Kitanidis 1994; Nordin and Sabol 1974; Mull et al. 1988). Using field data, these relationships have often been used to demonstrate that the ADE fails to explain empirical tracer RTD, leading authors to reject the assumption of Fickian transport (Atkinson and Davis 2000; Le Borgne and Gouze 2008; Morales et al. 2007).

Given initial and boundary conditions, fundamental solutions to the ADE can be regarded as impulse responses $h(t)$ of the system, which gives the RTD of tracer particles (Lepiller and Mondain 1986). Various solutions to the ADE can be given depending on the boundary conditions, i.e. the type of injection and detection mode (Kreft and Zuber 1978). The two most used solutions are those using injection and detection in fluid flux or resident fluid for an instantaneous release of tracer, denoted C_{IFF} and C_{IRR} respectively, following Kreft and Zuber (1978) notations. Resident fluid and fluid flux concentrations both refer to the mass of solute contained in a given volume of water. They differ in the way they express that volume of water; for resident concentrations it is an infinitesimally small stream tube at a given time, whereas for flux concentrations it is the product of the flux and an infinitesimally small period of time at a given location along the flow path. By definition, the use of "instantaneous injection" and "planar injection" mean that one is considering an injection in flux or resident fluid respectively (Kreft and Zuber 1978). As shown by many authors (e.g. Carlier 2008; Kreft and Zuber 1978; Parker and van Genuchten 1984; Zuber 1983), the use of flux concentration is of great interest for the interpretation of most dye tracing experiments. An analytical solution to the ADE assuming resident concentration is however often used. The corresponding analytical solutions are given by Eq. (4):

$$\begin{cases} C_{\mathrm{IRR}} : h(t) = \dfrac{V}{\sqrt{4\pi D t}} e^{\frac{-(\ell - Vt)^2}{4Dt}} \\ C_{\mathrm{IFF}} : h(t) = \dfrac{\ell}{t\sqrt{4\pi D t}} e^{\frac{-(\ell - Vt)^2}{4Dt}} \end{cases} \tag{4}$$

In Eq. (4), the main sought parameters of $h(t)$ at the detection point $x = \ell$ are the mean residence time of water t_{mean}, the peak arrival time or modal time t_{mod} and the maximum value or mode h_{mod}. The modal time of the tracer and the corresponding mode are more useful for risk assessment, while the mean residence time of water is related to the flow velocity, and has consequently more meaning hydraulically (Field and Nash 1997).

At the detection point $x = \ell$, the mean residence time of water (t_{mean}) is the ratio ℓ/V. The position $x = \ell$ at which all the hydrodispersive parameters are determined defines the length of the flow path, and thus the scale of the tracing system through which the tracer is transported. The mean residence time of the tracer is given by the first time-moment of $h(m_{1t})$, which equals t_{mean} for the C_{IFF} case only (Kreft and Zuber 1978). For the C_{IRR} case, t_{mean} can be expressed as a function of Pe and m_{1t} (Eq. 5).

$$\begin{cases} C_{\mathrm{IFF}} : t_{\mathrm{mean}} = m_{1t} \\ C_{\mathrm{IRR}} : t_{\mathrm{mean}} = \dfrac{\mathrm{Pe} + 2}{\mathrm{Pe}} m_{1t} \end{cases} \tag{5}$$

Theoretical relationships between parameters

The relationships between modal (t_{mod}) and mean residence time of a tracer (m_{1t}) is given by Eq. (6) (Wang and Crampon 1995; Singh 2006):

$$t_{\mathrm{mod}} = m_{1t} \times k \text{ with } \begin{cases} C_{\mathrm{IRR}} : k = \sqrt{\left(\dfrac{1}{\mathrm{Pe}}\right)^2 + 1} - \dfrac{1}{\mathrm{Pe}} \\ C_{\mathrm{IFF}} : k = \sqrt{\left(\dfrac{3}{\mathrm{Pe}}\right)^2 + 1} - \dfrac{3}{\mathrm{Pe}} \end{cases} \tag{6}$$

Equation (5) shows that there is a proportional relationship that relates the modal time to the mean residence time of a tracer for both cases of injection/detection modes. This

dimensionless proportionality factor is denoted as k. Its value can be interpreted as a measure of the asymmetry of the RTD and varies between 0 (when Pe tends towards 0) and 1 (when Pe tends towards $+\infty$).

The mode of the RTD can be computed at the position $x = \ell$ using the partial derivative of $h(t)$ according to time (Eq. 4), which has to be zero for $t = t_{\mathrm{mod}}$. Equation (7) gives the analytical expressions of the mode of $h(t)$ for C_{IFF} and C_{IRR} cases:

$$\begin{cases} C_{\mathrm{IRR}} : h_{\mathrm{mod}} = \dfrac{p}{t_{\mathrm{mod}}} \text{ where } p = \sqrt{\dfrac{k\mathrm{Pe}}{4\pi}} \times e^{\frac{-\mathrm{Pe}(1-k)^2}{4k}} \\ C_{\mathrm{IFF}} : h_{\mathrm{mod}} = \dfrac{p}{t_{\mathrm{mod}}} \text{ where } p = \sqrt{\dfrac{\mathrm{Pe}}{4\pi k}} \times e^{\frac{-\mathrm{Pe}(1-k)^2}{4k}} \end{cases} \quad (7)$$

Equation (7) shows that the mode of the RTD is inversely proportional to the arrival time of the peak concentration. This proportionality factor is denoted as p and is called the peak/time factor. Its analytical expression is relatively complex, but tends towards the ratio $(\mathrm{Pe}/4\pi)^{1/2}$ for a large Pe. The error on the evaluation of p is less than 5% for $\mathrm{Pe} > 15$, i.e. when advection dominates transport processes.

The k (Eq. 6) and p (Eq. 7) proportionality factors are functions of the Peclet number only. The validity of these linear relationships is checked in the next section using a large database of tracer RTD parameters for various hydrological and hydrogeological contexts.

Experimental validation

Tracer RTD database

Jobson (1997) described a large dataset of tracer RTDs conducted in surface streams that can be found in Jobson (1996); these works gathered a great compilation of data that aimed to better predict travel time of solutes or contaminants in rivers. Later, Morales et al. (2007) provided a comparison with results involving tracer RTD parameters from tracer tests performed in karst aquifers. These values of tracer RTD parameters have been compiled and completed in the study reported here, using other data from the scientific literature, including scientific reports from metric to kilometric scales. Only a few of them were selected, according to the following rules:

- Flow condition should be known and stable during the test.
- Mass recovery and peak concentration must be known.
- Sampling resolution must be consistent with the recovery dynamics.
- Position of injection and detection points must be known, with a basic geological description (at least the nature of the aquifer).
- Multipeak recovery due to different flow paths are not taken into account.

No matter the type of test that is carried out, the actual pathway travelled by the tracer remains difficult or even impossible to know over long distances, and the assumptions inherent in the application of a 1D scheme of the transport equation will be always questionable. As a result, it was chosen to keep the results from tracer experiments performed in radial flow, knowing that they can be approximated by Eq. (4) with a relatively small error (Wang and Crampon 1995).

The resulting database gives the main characteristics of RTDs from 583 tracer tests, from a few meters to over 30 km long, in four types of media: karst aquifer, fractured aquifer, surface stream, and water column with hydraulic restriction (laboratory experiment, Dzikowski et al. 1991). This database is given in Table S1 of the electronic supplementary material (ESM).

Data interpretation

The full database can be divided into three parts: (1) results from various tracer tests carried out on the same tracing system, thus at a fixed scale but for differing hydrological states, (2) results from one tracer test with detection at different positions along the flow path, and (3) results from the whole database, including cases 1 and 2. This third part is referred to as the "general case" in the following.

Fixed scale

In the first case, the scale ℓ of the tracing system is fixed, but the flow velocity varies from one test to another. This type of experiment is typically performed on karst systems to better qualify the vulnerability of a given infiltration point in various hydrologic conditions. In all, 34 tracer tests performed on 8 tracing systems from different karst aquifers were used to illustrate the case of a fixed scale in various hydrologic conditions: 7 tracer tests with recovery observed at Dyers Spring in USA (Mull et al. 1988), 3 at the Rinquelle spring in Switzerland (Leibundgut 1998), 2 from the Pont de Pierre karst system in France in very different hydrological conditions (Mondain 1989), 6 at the Rekalde spring in Spain (Morales et al. 2007), 5, 4 and 2 at Glassac, Boundoulaou and Dragonnière springs respectively, in the Grands-Causses area in France (de la Bernardie 2013), and 5 from the Bange-l'Eau Morte karst system in France (Lepiller 2001) for which the mean residence time is used as an approximation of the modal time, the latter being unknown. Figure 1 shows a logarithmic plot of h_{mod} as a function of t_{mod} from these tracer tests. One can notice that the results for a given tracing systems fall along a specific line defined by a constant Pe value. These lines are computed using Eq. (7) for C_{IFF} conditions, which means that the peak of concentration can be reproduced using the same Pe number for a given tracing system.

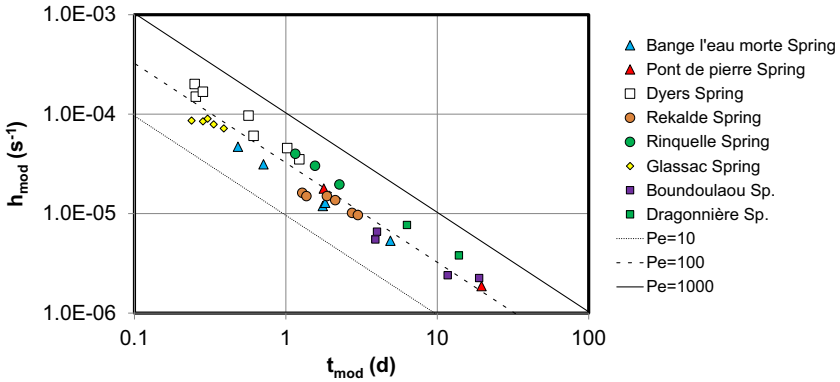

Fig. 1 Case of a fixed scale. Results from eight tracing systems compared to theoretical relationships between h_{mod} and t_{mod} for Pe values ranging from 10 to 1,000

Fixed flow velocity

In the second case, the scale ℓ of the tracing system increased between successive stations along the flow path, but the flow velocity is assumed to be constant and uniform. Previous works showed that the relationship between the mode of the RTD and the modal time should follow a power law $h(t) \propto t^b$, with an exponent $b = -½$ if the dispersivity does not vary with the scale (e.g. Davis et al. 2000; Jobson 1997; Kitanidis 1994; Nordin and Sabol 1974). This equation should however only be applied to relate the mode of the spatial distribution of the resident concentration to the modal time. It can however be used as a good approximation of the relationship between the mode of the RTD and the modal time for a large Pe, as it occurs in surface streams and channels.

Tracer tests for distances travelled, which increased throughout the study, were typically done in rivers and channels to better characterize the downstream dispersion of a contaminant. Four multistation tracer tests performed in surface streams were used to illustrate the time evolution of the mode of the RTD: The Severn River (UK) test with seven stations (Atkinson and Davis 2000) ranging from 210 to 13,375 m from the injection point, the Copper Creek (USA) with six stations ranging from 200 to 4,100 m (Jobson 1996), the Coachella Canal (USA) with six stations ranging from 300 to 5,100 m (Jobson 1996) and the Orb River (South France) with four stations ranging from 50 to 13,900 m from the injection (personal data).

Figure 2 shows a logarithmic plot of h_{mod} as a function of t_{mod} from these tracer tests. Once again, one can notice that the results for a given tracing system fall along a specific line defined by a constant Pe value (Eq. 7) for C_{IFF} conditions. If measurements are taken too early in the experiment, there can be issues resulting from a lack of homogenization from insufficient mixing of the tracer, as well as limited sampling frequencies. These, in addition to flow velocity variations along the river at later times may explain some of the discrepancies regarding the theoretical lines defined by a constant value for Pe.

It is obviously difficult to perform this type of experiment for tracing groundwater flow. Adams and Gelhar (1992) used a dense network of piezometers to describe the displacement of a tracer plume in three dimensions according to time through the MADE aquifer. Benson et al. (2001) used this dataset to discuss the ability of a fractional advection-dispersion equation to reproduce the tracer plume. This experiment can also be interpreted as another example of tracer tests where the scale ℓ of the tracing system increases from one piezometer to another along the flow path. It is shown in these works that the maximum bromide concentration follows a power-law relationship according to time. The plot of the maximum bromide concentration versus time in a logarithmic scale gives a slope between −0.9 and −1.05 according to data post-treatments, which perfectly fits the inverse relationship between the maximum value of the RTD and time. All these results demonstrate that the use of a linear relationship between scale and dispersivity allows a better understanding of the space and time evolution of the mode of the RTD.

General case

Previous results show that an inverse relationship between h_{mod} and t_{mod} is observed in experimental data when the scale of the tracer test or the flow velocity is fixed. This means that the Pe value can be deduced from any tracer test providing that h_{mod} and t_{mod} are known. Thus, each tracer test can be interpreted independently, i.e. without considering that scale or flow velocity is fixed from one test to another. This allowed all the results from the whole tracer database to be plotted on the same graph (Fig. 3).

The diagram shown in Fig. 3 represents a simple approach of tracer test diagnosis, which is called h_{mod}/t_{mod} diagnosis in the following. Previous results demonstrate that an inverse relationship exists between h_{mod} and t_{mod} according to the hydrodispersive properties (Pe) of each tracing system. As a result, a straight line of slope, –1 in the h_{mod} vs. t_{mod} diagram, can be used to assess the Pe for each tracing system. This diagram is based on the assumption of C_{IFF} conditions, knowing that the use of C_{IRR} conditions will only affect the characteristic lines for a Pe lower than 10. Most tracer tests carried out in surface streams are characterized by Pe values from 100

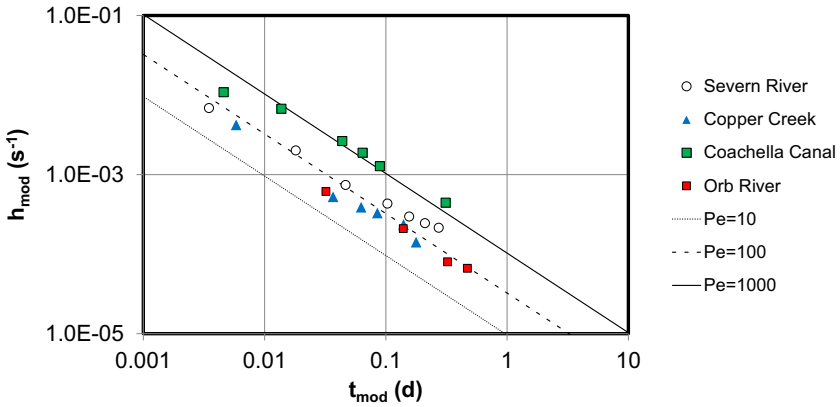

Fig. 2 Case of constant hydrological conditions. Results from four multistation tracer tests along a surface stream compared to theoretical relationships between h_{mod} and t_{mod} for Pe values ranging from 10 to 1,000

to 1,000, while Pe values of tests carried out in karst systems are a bit lower and range from 10 to few hundred. Pe values in fractured rocks are significantly lower, and can be as low as one.

A linear relationship between modal time and mean residence time is also expected following Eq. (6). Figure 4 shows the results assuming C_{IFF} conditions for tracer tests performed in karst aquifers ($n = 97$). No information about the mode of the RTD is required. Figure 4 shows that most tracer tests performed in karst systems are characterized by a Pe higher than 10, which is consistent with the previous results (Fig. 3), but this diagram does not allow a clear determination of the Pe value.

Discussion and implication for tracer test design and interpretation

Inverse relationship between h_{mod} and t_{mod}

This new approach has been applied to a large dataset of tracer tests mostly carried out in surface waters and karst or fractured groundwater systems. No information was available at a large scale for porous aquifers to apply this approach. Results from the MADE tracer tests (Adams and Gelhar 1992) have been used to validate the inverse relationship between mode and modal time of the RTD in a heterogeneous porous aquifer. In addition, factors ranging from 0.041 to 0.256 (0.1 on average) between macro-dispersivity and scale were found by Pickens and Grisak (1981) in a stratified granular aquifer. Following Eq. (3), these values correspond to a Pe ranging from 4 to 24 (10 on average), which is an intermediate value between fractured media and karst aquifers (Fig. 3).

Using regression analysis, Jobson (1996) and Morales et al. (2007) found power coefficients $b = -0.89$ and $b = -0.85$, respectively, to describe the evolution of the mode of the RTD with time in karst systems. These results were interpreted by the authors as evidence of non-Fickian behavior. Accordingly, Fig. 3 could also be used to fit power-law relationships relating h_{mod} to t_{mod}. Primarily, this interpretation prevents the assessment of the Peclet number using Eq. (7), and another theory should be used to characterize transport processes. This would also mean for instance that all tracing systems performed in karst aquifers could be characterized by the same power-law relationship. There is however a bias in this interpretation when various tracing systems are brought together: the more advection dominates the solute transport processes, the easier it is to perform tracer tests over very long distances, and therefore with relatively long residence times. This sampling bias causes a positive trend between Pe and t_{mod}, which

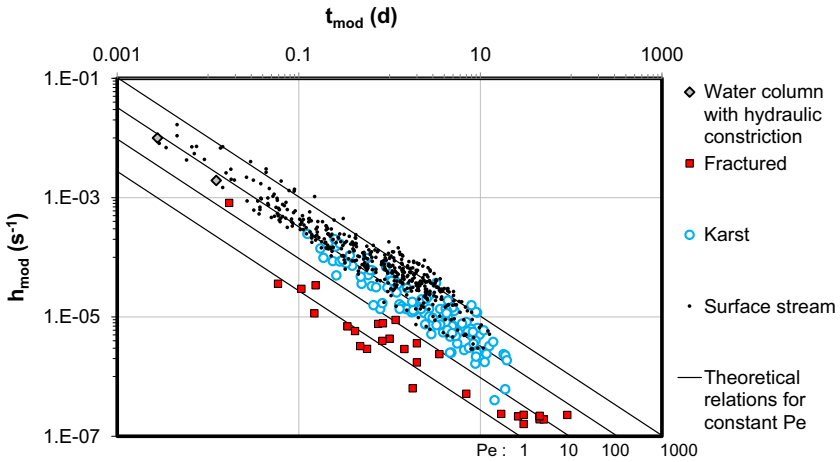

Fig. 3 h_{mod}/t_{mod} diagnosis performed on the whole tracer test database ($n = 583$) with theoretical relations given by constant Pe assuming C_{IFF} conditions

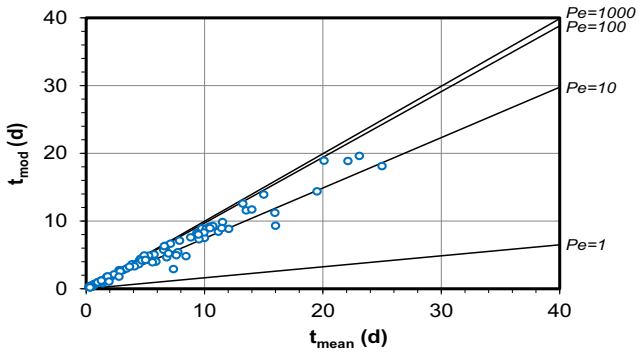

Fig. 4 t_{mod}/t_{mean} diagnosis performed on karst aquifer systems ($n = 97$)

can explain why the fit of a power-law relationship related to surface streams, karst or fractured media in Fig. 3 will result in a power coefficient slightly lower than 1 (−0.88, −0.92, −0.85 respectively). This bias is not identified for a given tracing system (Fig. 1), which supports this interpretation.

Another explanation for the spreading of points in Fig. 3 comes from the use of a global characterization of hydrodispersive parameters of the tracing system. If the latter consists of an injection zone with distinct hydrodispersive parameters such as a thick infiltration zone, or a mixing in the water column in an injection well, the residence time distribution of the tracer within this first tracing subsystem should be taken into account. Considering the tracing system as a whole may, thus, introduce another bias in the analysis according to the relative importance of transport processes in each tracing subsystem encountered by the tracer cloud. This should however not be correlated to t_{mod}, and thus not introduce any trend in Fig. 3, but it can explain some noise in the relationships.

Finally, the interpretation of tracer tests performed in fractured media in Fig. 3 gives a Pe value close to 1, which means that hydrodynamic dispersion dominates the solute transport processes. For such low values, the interpretation of Pe based on the h_{mod}/t_{mod} diagnosis is very sensitive to the initial boundary conditions, i.e. the injection mode in resident or flux concentration, but also to the dilution procedure that is used for well injection, which is the most common procedure for tracer test performed in fractured media. Different protocols of tracer test could thus explain a greater variability in results for this type of media.

Worthington and Smart (2003, 2011) used their own tracer database of 195 tracer tests to propose various empirical relationships that can be used to assess the mass to be injected. Among them, one significant relationship previously proposed by Dole (1906) is of the form:

$$M = A \times \left(t_{mod} \times Q \times C_{peak}\right)^{B} \quad (8)$$

where A and B are two fitted parameters, M (g) is the injected mass of the tracer, Q (m^3/s) is the discharge and C_{peak} (g/m^3) is the peak of concentration at the detection point. According to Worthington and Smart (2011), with a correlation coefficient of 0.96, Eq. (8) gives $A = 0.84$ and $B = 0.96$. The latter being really close to 1, Eq. (8) can consequently be re-written using $B = 1$, which gives:

$$\frac{Q \times C_{peak}}{M} \cong \frac{1}{0.84 \times t_{mod}} \quad (9)$$

Assuming permanent flow conditions and neglecting the effect of partial mass recovery, the left side of Eq. (9) is precisely the analytical expression of h_{mod}, which appears as inversely proportional to t_{mod} with a Pe close to 20 using Eq. (7). These examples show how previous empirical relationships found between parameters of RTDs support the assumption of an inverse relationship between h_{mod} and t_{mod}. All these results suggest that the Peclet number can be seen as an intrinsic parameter of the dispersive media for large-scale contaminant transport studies, which leads to an inverse relationship between the mode and the modal time of the RTD.

Application for tracer test design and interpretation

Tracer test design

This approach was used to design two tracer tests which were performed in May 2015 (T1) and March 2018 (T2) on the Plateau de Sault in the French Pyreneans (Bailly-Comte et al. 2018). The tracer was injected into the same sinking stream called “les Taillades” at the “Rebounedou” sinkhole, around 13 km west of the Fontmaure karst spring (BSS002MGKH, 42°50′34″ N, 2°12′10″ E), where it was supposed to flow out.

A Pe value of 100 was chosen as a typical value for a karst tracing system (Fig. 3), which gives $k = 0.97$ (Eq. 6) and a peak/time factor $p = 2.80$ (Eq. 7) for C_{IFF} conditions. These tracer tests were planned for spring discharge around 2 and 5 m^3/s respectively, with an expected maximum concentration of 10 ppb. The first tracer test T1 was done in medium-flow conditions, for which a flow velocity of 40 m/h was chosen considering typical values for tracer tests injected in active sinking streams. The second experiment T2 was done in high flow conditions so that a flow velocity close to 100 m/h could be expected. The actual scale ℓ of the tracing system is unknown, so the shortest distance between the sinkhole and the spring (13 km) was used for the T1 and T2 experiments. The tracer recovery R (%) is also mandatory. It is assumed to be 70%. The mass M (g) of tracer to be injected can then be computed with Eq. (10) assuming C_{IFF} conditions, where C is the expected maximum concentration of tracer (C = 10 ppb):

$$M = \frac{\ell Q C k}{R p} \quad (10)$$

This relationship gives a mass to be injected of 11.6 kg for T1 and T2, because the changes of Q are compensated by the changes of V. This approach gives an order of magnitude that should be compared to other case studies in similar settings. A mass of 10 kg was used for T1 (sulforhodamine) and T2 (uranine). The maximum measured concentration using a GGUN fluorometer (Manufacturer: Albillia SARL, Lemke et al. 2013) was 8.03 and 10.08 ppb respectively (Fig. 5), with a recovery of 104 and 74%.

h_{mod}/t_{mod} method for hydrodispersive parameter determination

The main characteristics of the T1 and T2 RTD are given in Table 1, including travel time skewness (Mull et al. 1988) and kurtosis (Field 2002). Tracer travel time skewness is a measure of the lateral asymmetry of the RTD, while the kurtosis characterizes the flattening of the signal relative to the peak. These two dimensionless parameters are useful for the interpretation of multiple tracer tests conducted under differing hydrologic conditions from the same injection points to the same recovery locations, as described by Mull et al. (1988) and Field (2002). In this study, there were only very slight changes in skewness and kurtosis from T1 to T2, with no significant differences. This means that the corresponding standardized RTD should be very similar, and that a composite curve which represents the typical shape of the two standardized dye-trace curves could be drawn following the method by Mull et al. (1988).

Table 1 and Eq. (7) can be used for the assessment of p as the product of h_{mod} and t_{mod}. Then, the simplification of Eq. (7) for a large Pe can be used for a first assessment of Pe, which gives Pe = 75 and Pe = 117 for T1 and T2 respectively. These values are high enough that it is not necessary to solve the complete equation. The value of k can be computed following Eq. (6) assuming C_{IFF} or C_{IRR} conditions, as well as the corresponding mean residence time of the tracer. The corresponding mean residence time of water is then computed following Eq. (5), which in turn is used to compute the flow velocity V. This method allows the determination of hydrodispersive parameters for C_{IFF} and C_{IRR} conditions that are numerically identical, using the same Peclet number but a slightly different value of V. The results are given in Table 1, and the corresponding curves are shown on Fig. 5 for T1 and T2 respectively. As a comparison, the results given by the Chatwin (1971) method using QTRACER2 (Field 2002), which assumes C_{IRR} conditions, and the method of moments (Maloszewski and Zuber 1992), which assumes C_{IFF} conditions, are also reported in these figures and in Table 1.

If both the method of moments and the Chatwin (1971) method allow the observed mean residence time of water to remain in the simulation (Table 1), they fail to reproduce the whole dynamics of the RTD, and especially the timing of the peak. The new h_{mod}/t_{mod} method better reproduces the complete dynamics and, by definition, the peak magnitude and timing (Fig. 5). The inherent assumptions, and especially those regarding uniform and constant flow velocity along the flow path, prevent the obtainment of a good reproduction of late time recovery, meaning that the first arrival of the tracer will be overestimated, while late time recovery will be underestimated. However, given the simplicity of the approach, the results fully fit the need for a better simulation of large-scale transport when considering simulations of pollution scenarios or vulnerability assessments on accidental pollution (Cornaton et al. 2004; Dedewanou et al. 2015; Jeannin et al. 2001; Popescu et al. 2019).

Each method gives Pe values that are of the same order of magnitude for T1 and T2 (Table 1), which is consistent for two tracers tests carried out through the same tracing system. Another way to describe the typical shape of the RTD according to hydrologic conditions is to represent the h_{mod}/t_{mod} theoretical relationship that best fits the two RTD, and to use it as

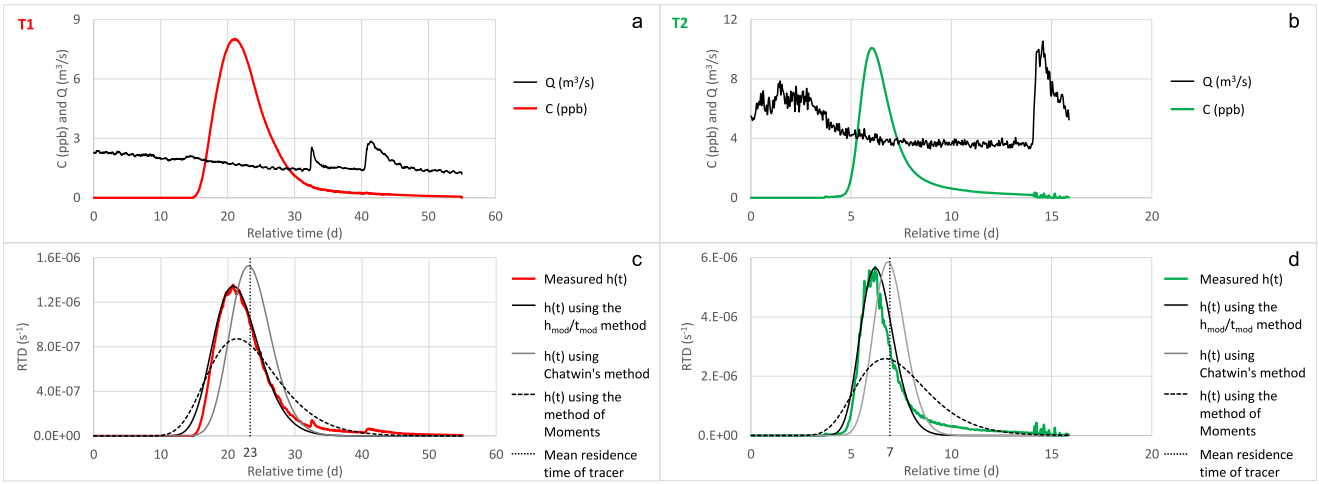

Fig. 5 Discharge and concentration time series (**a**–**b**) and results of RTD simulation (**c**–**d**) for the T1 and T2 tracer tests

Table 1 Main characteristics of the T1 and T2 residence time distribution (RTD) with results from the h_{mod}/t_{mod}, Chatwin (1971) and moments (Maloszewski and Zuber 1992) methods for the determination of hydrodispersive parameters

Test	RTD characteristics							h_{mod}/t_{mod} C_{IFF}		h_{mod}/t_{mod} C_{IRR}		Chatwin C_{IRR}		Moments C_{IFF}	
	C_{peak} (ppb)	t_{mean} (days)	t_{mod} (days)	h_{mod} (10^6 s^{-1})	V (m/h)	Skewness [–]	Kurtosis [–]	Pe [–]	V (m/h)	Pe [–]	V (m/h)	Pe [–]	V (m/h)	Pe [–]	V (m/h)
T1	8.03	23.3	20.8	1.36	23.23	2.1	9.0	75	25.03	75	25.04	118	23.29	34	23.23
T2	10.08	6.9	6.2	5.69	78.13	2.2	8.2	117	85.14	117	85.15	152	78.71	30	78.13

an envelope curve for peak concentration prediction (Fig. 6). A value of Pe = 80 ± 20 was chosen, given the results of the h_{mod}/t_{mod} method. The diagram shown on Fig. 6 can be used to assess the magnitude of pollution at this spring for various hydrological conditions, providing that the corresponding flow velocity, and thus t_{mean} and t_{mod}, can be known from discharge measurements. The same method could be applied to the tracer RTD used in Fig. 1. The uncertainty on the estimation of the envelope curve can be reduced by carrying out numerous tracer tests on the same site in differing hydrological conditions, taking into account other uncertainties resulting from tracer concentration and discharge measurements. According to Eq. (7), the differences between two envelope curves is proportional to the p variation, but also inversely proportional to time, which means that short modal time allows a better identification of the Pe value for a given tracing system.

Conclusion

This work shows how a linear-scale effect in dispersive media can be implemented in a 1D advection-dispersion framework for a better representation of large-scale transport processes. For this purpose, a database of tracer tests has been set up and used for the validation of analytical relationships between hydrodispersive parameters, especially the ones that link Pe, h_{mod} and t_{mod}. Results based on 583 tracer tests show that Pe can be used as an intrinsic parameter of the tracing system, without scale-dependence. Other empirical relationships found in previous studies are also used to support these conclusions, providing new insights into their statistical interpretations.

A new approach based on a new peak/time factor, i.e. the inverse relationship between the mode of the RTD, or peak concentration and time is proposed for RTD prediction (tracer test design) and simulation (hydrodispersive parameters estimation). The results from two tracer tests are compared to other simple but well-recognized methods of tracer test breakthrough curve analyses. The results show that the h_{mod}/t_{mod} method is more efficient if one is focused on magnitude and arrival time of peak concentration, while it tends to underestimate the tracer mean residence time. In addition, the h_{mod}/t_{mod} diagnosis in a logarithmic plot gives interesting perspectives for simple approaches of transport modeling, especially for vulnerability mapping or protection zone delineation, which need very parsimonious approaches to predict the transport of contaminants. This method can also be used to predict the changes in RTD under different hydrological conditions: the typical envelope curve of the h_{mod}/t_{mod} relationships can be drawn for a given tracing system, under which all RTDs can be computed according to flow velocity.

This analysis focused on the peak of the RTD and cannot be used to predict complex retardation and other tailing effects or a multipeak recovery due to complex flow geometries, as other simple methods based on 1D ADE. It is also limited to permanent and uniform flow conditions, except if some mathematical treatments can be done prior to the h_{mod}/t_{mod} diagnosis (Carlier 2008).

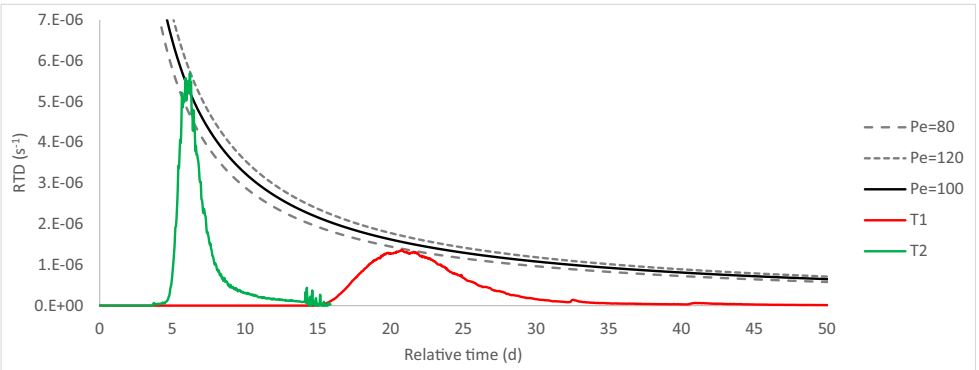

Fig. 6 Example of envelope curves for peak concentration prediction determined from T1 and T2 tracer tests

Further statistical investigation should be performed using a more comprehensive database of tracer RTD parameters obtained under permanent flow conditions to better characterize the sensitivity of Pe values to hydrogeological characteristics of the tracing system. Its sensitivity to recharge dynamics should also be investigated, especially when soils or a thick unsaturated zone may play an important role in kinematic dispersion. This is particularly true for karst aquifers since the type of infiltration through sinking streams, dolines or other epikarst features could play a relevant role. Such information should be available through the numerous data-sharing initiatives in the scientific community, like for example the BD Tracage project in France.

Supplementary Information The online version contains supplementary material available at https://doi.org/10.1007/s10040-021-02327-x.

Acknowledgements We would like to thank the HydroSciences laboratory for the use of the tracer test data from the Orb River, B. Vayssade for his helpful comments and all the numerous contributors to the tracer RTD parameter database. We also acknowledge the Adour-Garonne water agency for the funding of the hydrogeological study of the Sault Plateau and speleologists from CDS09 and CDS11 that were involved in the tracer test experiments.

References

Adams EE, Gelhar LW (1992) Field study of dispersion in a heterogeneous aquifer: 2. spatial moments analysis. Water Resour Res 28(12):3293–3307. https://doi.org/10.1029/92WR01757

Atkinson TC, Davis PM (2000) Longitudinal dispersion in natural channels: l. experimental results from the River Severn, U.K. Hydrol Earth Syst Sci 4(3):345–353

Bailly-Comte V, Ladouche B, Allanic C, Bitri A, Moiroux F, Monod B, Vigouroux Ph, Maréchal JC, Grandemange A, Bardeau M, Tilloloy F (2018) Evaluation des ressources en eaux souterraines du Plateau de Sault: amélioration des connaissances sur les potentialités de la ressource et cartographie de la vulnérabilité [Assessment of groundwater resources in the Sault Plateau: knowledge improvement on the potentialities of the resource and mapping of vulnerability]. Final report, BRGM/RP-67528-FR, BRGM, Orléans, France, 305 pp, http://ficheinfoterre.brgm.fr/document/RP-67528-FR

Bear J (1972) Dynamics of fluids in porous media. Elsevier, New York, 764 pp

Becker MW, Shapiro AM (2003) Interpreting tracer breakthrough tailing from different forced-gradient tracer experiment configurations in fractured bedrock. Water Resour Res 39(1):1024. https://doi.org/10.1029/2001wr001190

Benson DA, Schumer R, Meerschaert MM, Wheatcraft SW (2001) Fractional dispersion, Levy motion, and the MADE tracer tests. Transport Porous Media 42:211–240

Berkowitz B, Cortis A, Dentz M, Scher H (2006) Modeling non-Fickian transport in geological formations as a continuous time random walk. Rev Geophys 44:RG2003. https://doi.org/10.1029/2005RG000178

Birk S, Geyer T, Liedl R, Sauter M (2005) Process-based interpretation of tracer tests in carbonate aquifers. Groundwater 43:381–388. https://doi.org/10.1111/j.1745-6584.2005.0033.x

Carlier E (2008) Analytical solutions of the advection-dispersion equation for transient groundwater flow. Numer Valid Hydrol Process 22(17):3500–3506

Chatwin PC (1971) On the interpretation of some longitudinal dispersion experiments. J Fluid Mech 48(4):689–702

Cornaton F, Goldscheider N, Jeannin P-Y, Perrochet P, Pochon A, Sinreich M, Zwahlen F (2004) The VULK analytical transport model and mapping method. In: Vulnerability and risk mapping for the protection of carbonate (karst) aquifers, pp. 155-160. Final report (COST Action 620), COST, Brussels

Cvetkovic V (2013) How accurate is predictive modeling of groundwater transport? A case study of advection, macrodispersion, and diffusive mass transfer at the Forsmark site (Sweden). Water Resour Res 49:5317–5327. https://doi.org/10.1002/wrcr.20429.

Davis PM, Atkinson TC, Wigley TML (2000) Longitudinal dispersion in natural channels: 2. the roles of shear flow dispersion and dead zones in the River Severn, U.K. Hydrol Earth Syst Sci 4(3):355–371

de Marsily G (1986) Quantitative hydrogeology: groundwater hydrology for engineers. Academic Press, Inc., Harcourt Brace Jovanich Publishers, 464 pp

de la Bernardie (2013) Etude de la relation entre débits des sources karstiques et distributions des temps de séjour [Study of the relationship between flows of karst sources and distribution of residence times]. MSc Thesis, Université Pierre et Marie Curie, Paris, 50 pp

Dedewanou M, Binet S, Rouet JL, Coquet Y, Bruand A, Noel H (2015) Groundwater vulnerability and risk mapping based on residence time distributions: spatial analysis for the estimation of lumped parameters. Water Resour Manag 29:5489–5504. https://doi.org/10.1007/s11269-015-1130-8

Dole RB (1906) Use of fluorescein in the study of underground waters, in Fuller, M.L., Underground-water papers, 1906. U.S. Geological Survey Water-Supply Paper 160, p. 73-85

Dzikowski M, Carlier E, Crampon N, de Marsily G (1991) Relations entre réponses impulsionnelles et conditions hydrodynamiques des systèmes dans le cadre de traçages artificiels: Theorie et application sur colonne de laboratoire [Relations between impulse responses and hydrodynamic conditions of systems in the context of artificial tracings: theory and application on laboratory column]. J Hydrol 125(1–2):129–148. https://doi.org/10.1016/0022-1694(91)90087-X.

Fadili A, Ababou R, Lenormand R (1999) Dispersive particle transport: identification of macroscale behavior in heterogeneous stratified subsurface flows. Math Geol 31(7):793–840

Fetter CW (1992) Contaminant hydrogeology. MacMillan, New York, 458 pp

Field MS (2002) The Qtracer2 program for tracer-breakthrough curve analysis for tracer tests in karstic aquifers and other hydrologic systems. U.S. Environmental Protection Agency, Office of Research and Development, National Center for Environmental Assessment, Washington Office, Washington, DC, EPA/600/R-02/001, 2002

Field M, Nash S (1997) Risk assessment methodology for karst aquifers: (1) estimating karst conduit-flow parameters. Environ Monit Assess 47:1–21

Fisher HB (1967) The mechanics of dispersion in natural streams. J Hydrol Div ASCE 93(6):187–216

Gelhar LW, Welty C, Rehfeldt KR (1992) A critical review of data on field-scale dispersion in aquifers. Water Resour Res 28(7):1955–1974. https://doi.org/10.1029/92wr00607

Huang K, van Genuchten MT, Renduo Z (1996) Exact solutions for one-dimensional transport with asymptotic scale-dependent dispersion. Appl Math Modelling 20(4):298–308. https://doi.org/10.1016/0307-904X(95)00123-2

Jeannin P-Y, Cornaton F, Zwahlen F, Perrochet P (2001) Vulk: a tool for intrinsic vulnerability assessment and validation. 7th Conference on Limestone Hydrology and Fissured Media, Besançon, France, 20–22 September 2001, pp 185–190

Jobson HE (1996) Prediction of travel time and longitudinal dispersion in Rivers and streams. US Geol Surv Water Resour Invest Rep 96-4013, 30 pp

Jobson HE (1997) Predicting travel time and dispersion in rivers and streams. J Hydraul Eng 123(11):971–978

Kitanidis PK (1994) The concept of the dilution index. Water Resour Res 30(7):2011–2026

Kreft A, Zuber A (1978) On the physical meaning of the dispersion equation and its solutions for different initial and boundary conditions. Chem Eng Sci 33(11):1471–1480

Labat D, Mangin A (2015) Transfer function approach for artificial tracer test interpretation in karstic systems. J Hydrol 529(3):866–871. https://doi.org/10.1016/j.jhydrol.2015.09.011

Lallemand-Barres A, Peaudecerf P (1978) Recherche des relations entre la valeur de la dispersivité macroscopique d'un aquifère, ses autres caractéristiques et les conditions de mesure [Investigation of the relationships between the value of the macroscopic dispersion of an aquifer, its other characteristics and the measurement conditions]. Bull BRGM 3(4):277–284

Lauber U, Goldscheider N (2014) Use of artificial and natural tracers to assess groundwater transit-time distribution and flow systems in a high-alpine karst system (Wetterstein Mountains, Germany). Hydrogeol J 22:1807–1824. https://doi.org/10.1007/s10040-014-1173-6

Le Borgne T, Gouze P (2008) Non-Fickian dispersion in porous media: 2. model validation from measurements at different scales. Water Res 44(6):W06427

Leibundgut C (1998) Vulnerability of karst aquifers. Karst hydrology. In: Proceedings of workshop W2 held at Rabat, Morocco, April–May 1997, IAHS Publ. 247, IAHS, Wallingford, UK, http://hydrologie.org/redbooks/a247/iahs_247_0045.pdf

Lemke D, Schnegg P, Schwientek M, Osenbrück K, Cirpka OA (2013) On-line fluorometry of multiple reactive and conservative tracers in streams. Environ Earth Sci 69:349–358. https://doi.org/10.1007/s12665-013-2305-3

Lenormand R (1995) A stream tube model for miscible flow. Transp Porous Media 18(3):245–261

Lepiller M (2001) Traçages appliqués à la dynamique des aquifères: possibilités et limites [Tracer tests applied to the dynamics of aquifers: possibilities and limitations]. Géologues 129:79–84

Lepiller M, Mondain PH (1986) Les traçages artificiels en hydrologie karstique: mise en œuvre et interprétation [Tracer tests in karst hydrology: implementation and interpretation]. Hydrogéologie 1:32–52

Maloszewski P, Zuber A (1982) Determining the turnover time of groundwater systems with the aid of environmental tracers: 1. models and their applicability. J Hydrol 57(3–4):207–231

Maloszewski P, Zuber A, (1990) On the parameter estimation from artificial tracer experiments, ModelCARE 90: calibration and reliability in groundwater modelling. In: Proceedings of the conference held in the Hague, September 1990. IAHS Publ. no. 195, IAHS, Wallingford, UK, http://hydrologie.org/redbooks/a195/iahs_195_0053.pdf

Maloszewski P, Zuber A (1992) On the calibration and validation of mathematical models for the interpretation of tracer experiments in groundwater. Adv Water Resour 15:47–62

Massei N, Wang HQ, Field MS, Dupont JP, Bakalowicz M, Rodet J (2006) Interpreting tracer breakthrough tailing in a conduit-dominated karstic aquifer. Hydrogeol J 14:849–858. https://doi.org/10.1007/s10040-005-0010-3

Mondain PH, (1989) Hydrogéologie des systèmes karstiques de l'unité Delphino-helvétique inférieures entre les vallées du Fier et du Borne (Massif des Bornes, Haute-Savoie, France), [Hydrogeology of karst systems of the lower Delphino-Helvetic unit between the valleys of Fier and Borne (Massif des Bornes, Haute-Savoie, France)]. PhD Thesis, Laboratoire de Géologie Orléans, France, 254 pp. https://hal.archives-ouvertes.fr/tel-00784936/. Accessed March 2021

Morales T, de Valderrama IF, Uriarte JA, Antigüedad I, Olazar M (2007) Predicting travel times and transport characterization in karst conduits by analyzing tracer-breakthrough curves. J Hydrol 334(1–2):183–198

Morel-Seytoux HJ, Nachabe M (1992) An effective scale-dependent dispersivity deduced from a purely convective flow field. Hydrol Sci J 37(2):93–104

Mull DS, Liebermann TD, Smoot JL, Woosley LH (1988) Application of dye-tracing techniques for determining solute-transport characteristics of ground water in karst terranes. Technical report, PB-92-231356/XAB; EPA-904/6-88/001, Environmental Protection Agency, Atlanta, GA

Neuman S (1990) Universal scaling of hydraulic conductivities and dispersivities in geologic media. Water Resour Res 26(8):1749–1758

Nordin CF, Sabol GV (1974) Empirical data on longitudinal dispersion in rivers. US Geol Surv Water Invest Rep 74-20, pp. 332, https://pubs.usgs.gov/wri/1974/0020/report.pdf

Pang L, Hunt B (2001) Solutions and verification of a scale-dependent dispersion model. J Contam Hydrol 53(1–2):21–39

Parker JC, van Genuchten MT (1984) Flux-averaged and volume-averaged concentrations in continuum approaches to solute transport. Water Resour Res 20(7):866–872

Pickens JF, Grisak GE (1981) Scale-dependent dispersion in a stratified granular aquifer. Water Resour Res 17(4):1191–1211. https://doi.org/10.1029/WR017i004p01191

Popescu IC, Brouyère S, Dassargues A (2019) The APSÛ method for process-based groundwater vulnerability assessment. Hydrogeol J 27:2563. https://doi.org/10.1007/s10040-019-02013-z

Puyguiraud A, Gouze P, Dentz M (2019) Stochastic dynamics of Lagrangian pore-scale velocities in three-dimensional porous media. Water Resour Res 55(2):1196–1217. https://doi.org/10.1029/2018WR023702

Ronchetti F, Piccinini L, Deiana M, Ciccarese G, Vincenzi V, Aguzzoli A, Malavasi G, Fabbri P, Corsini A (2020) Tracer test to assess flow and transport parameters of an earth slide: the Montecagno landslide case study (Italy). Eng Geol 275. https://doi.org/10.1016/j.enggeo.2020.105749

Sauty JP (1980) An analysis of hydrodispersive transfer in aquifers. Water Resour Res 16:145–158

Schilling OS, Cook PG, Brunner P. (2019) Beyond classical observations in hydrogeology: the advantages of including exchange flux, temperature, tracer concentration, residence time and soil moisture observations in groundwater model calibration. Rev Geophys 57. https://doi.org/10.1029/2018RG000619

Schulze-Makuch D (2005) Longitudinal dispersivity data and implications for scaling behavior. Ground Water 43(3):443–456. https://doi.org/10.1111/j.1745-6584.2005.0051.x

Singh SK (2006) Estimating dispersivity and injected mass from breakthrough curve due to instantaneous source. J Hydrol 329(3–4):685–691

Wang HQ, Crampon N (1995) Method for interpreting tracer experiments in radial flow using modified analytical solutions. J Hydrol 165(1–4):11–31

Worthington SRH, Smart CC (2003) Empirical determination of tracer mass for sink to spring tests in karst. American Society of Civil Engineers, Geotechnical Special Publication, Sinkholes and the engineering and environmental impacts on karst. Washington, DC, pp 287–295, https://doi.org/10.1061/40698(2003)26

Worthington SRH, Smart CC (2011) Optimization of tracer mass for groundwater tracer tests in carbonate aquifers, H2Karst. Université de Franche-Comté - Université de Neuchâtel, Besançon, France, pp 487–490

Zuber A (1983) Tracer methods in isotope hydrology, models for tracer flow. IAEA, Vienna, pp 67–112